



DFT Modelling Studies of Spectroscopic Properties and Medium Effects on Molecular Reactivity of Secnidazole in Different Solvents

Ala Hssain ^{a, b} *^aUniversity of Halabja, College of Science, Department of Physics, Halabja, Iraq**^bFirat University, Department of Physics, Elazig, Turkey**Corresponding author: E-mail: ala.hssain@uoh.edu.iq*

ABSTRACT

The spectroscopic and optoelectronic investigations of (hydroxyl-2-propyl)-1-methyl-2-nitro-5-imidazole (secnidazole, C-7., H-11., N-3., O-3.) molecule were performed using C13 and H1 NMR chemical shifts and FT-IR spectroscopies. Molecular geometric optimizations, HOMO-LUMO properties, and molecular electrostatic potential (MPE) were studied using the B3LYP functional in the DFT method at the cc-pVDZ basis set. The UV-Vis spectra of the titled molecule in several solvents (water, dimethyl sulfoxide (DMSO), nitromethane, acetone, and tetrahydrofuran (THF)) were investigated theoretically with the aforementioned model method. The solvents have an effective role in the optoelectronic properties of the secnidazole molecule. From non-polar to polar solvents, the bandgap energy of secnidazole was found to be decreased for all of the solvents. Furthermore, the research aims at investigating the medium effects on solvation free energy, polarizability, dipole moment, first-order hyper-polarizability as well as several molecular properties such as chemical potential, electronegativity, chemical hardness and softness, and the electrophilicity index of secnidazole (SNZ). The aforementioned method and basis set were used for all kinds of computations in the gas phase and solution. The Solvation Model on Density (SMD) was applied to the aforementioned solvent systems to calculate the solvent polarity effect on the dipole moment, free energy, and molecular properties of the (SNZ) molecule. The free energies have gradually increased with a decrease in the solvent dielectric constant, i.e., as the solvent polarity decreases, the solvation energy increases. From polar to non-polar solvents, the dipole moment of secnidazole was found to be decreased. In various solvents, the dipole moment of secnidazole was greater than that of the gas phase. With the decrease of the solvent dielectric constant, the first-order hyperpolarizability and polarizability have also decreased. Besides, electronegativity, the chemical potential, and electrophilicity index decreased continuously from polar to non-polar solvents. Secnidazole's electronegativity, chemical potential, and electrophilicity index were higher in THF than in acetone. However, with increasing solvent polarity, chemical hardness decreased and the inverse relationship was noticed in the case of chemical softness. The obtained results in this computational investigation may lead to a better understanding of the stability and reactivity of secnidazole and will be helpful for the use of the title compound as reaction intermediates and pharmaceuticals.

ARTICLE INFO

Keywords:
Secnidazole

DFT
C¹³ and H¹ NMR
FT-IR
UV-Vis
Solvation Free Energy
SMD Model
Dipole moment
Polarizability

Received: 2022-03-24**Accepted:** 2022-04-15**ISSN:** 2651-3080**DOI:** 10.54565/jphcfum.1092855

1. Introduction

Secnidazole (SNZ) is known as an antimicrobial drug that can be used against some kinds of bacteria and parasites of anaerobicity, like trichomonas, giardia, and ameba, which are responsible for somewhat neglected diseases. It is named (hydroxyl-2-propyl)-1-methyl-2-nitro-5-imidazole (Figure 1) as stated by the classification of IUPAC. It is part of the chemical class of 5-nitro-imidazoles, and its structure is related to the tinidazole and metronidazole[1-4], that used against an assortment of G^+/G^- bacteria, but with severe side effects as to make use of it in high concentrations[5]. This medicine is provided as a white powder crystalline, and although it has been sold for a few decades, thus with a consolidated request, this active substance is not listed at all by the pharmacopeias. Secnidazole (SNZ) displays major degradation in the presence of light and under conditions of alkaline, though in neutral and acidic media extenuated. Several analytical techniques in pharmaceutical preparations have been published for determining secnidazole either alone or with other medicines [6, 7].

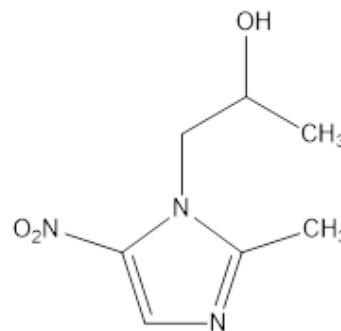
Secnidazole is an anhydrous solid that is unstable under standard conditions. Determinations of single-crystal structure display that this titled molecule crystallizes in the form of a hemihydrate and has two water molecules and four secnidazole molecules ($Z = 4$) per unit cell. Secnidazole hemihydrate is classed as the system of a monoclinic, space group $P2_1/c$, having ($a = 12.424 \text{ \AA}$, $b = 12.187 \text{ \AA}$, $c = 6.662 \text{ \AA}$, and $\beta = 100.9^\circ$)[8]. The molecules of water that are present in the structure that is shared amongst four half-occupied locations are also connected to a propyl radical resulting to form the hydrogen bonds of the formation of the head-tail. The molecules are kept together, and dimers are formed by a hydrogen bond between a molecule of water and the OH group [8]. Secnidazole has an interesting structure, since it has a nitro group and an OH group, which are powerful electron attracting and powerful electron-donating groups, respectively, and possess the possibilities of intermolecular and intramolecular hydrogen bonding as well. Many isomeric conformations can result in internal rotation around a C-C bond.

Experimentally, the thermal stability and polymorphism of secnidazole were studied by using X-ray powder diffraction, vibrational spectroscopy, and thermal analysis [9]. Quantum mechanical computations investigated the conformational stability of the titled molecule. Geometry optimizations were performed on the stable rotamers' possibilities. Comparisons were made with the correspondence relative energies. Combining infrared and Raman data with calculations of quantum mechanics, a comprehensive vibrational study of secnidazole was conducted. The traditional methods of study include Raman and Infrared spectroscopies and are especially effective for the characterization of non-destructive substances including living materials. Analysis of the computed vibrational spectra was done, based on the

potential energy distribution (PED) of each mode of vibration, which helped us to gain a qualitative as well as quantitative interpretation of the Raman and infrared spectra [8].

Variations in the polarity of solvents and the form of interaction(s) between solute-solvent can influence the geometry, hyper-polarizability, polarizability, dipole moment as well as properties of the molecule[10-12] because of changeable interactions between the highest occupied (HOMO) and lowest unoccupied molecular orbitals (LUMO) thus, the molecule's stability and reactivity can be affected[13, 14]. The characteristics of the molecule and interactions can be gained by Density Functional Theory (DFT) computations [15, 16], hence, the properties of the molecule will be well understood [17, 18].

Quantum mechanical computations for investigating the spectroscopic and stability of the titled molecule in different solvents are not found in the available data in the literature. Therefore, the current study was conducted theoretically to report the spectroscopic and optoelectronic properties of the SNZ molecule in several solvents as well as the solvent effect on free energy, polarizability, dipole moment and first-order hyper-polarizability of the secnidazole molecule as well as its chemical reactivity. This may be beneficial for a better understanding of the stability of the titled compound in various solvent systems and the production of (bio) chemical and new pharmaceutical products that are derived from SNZ.



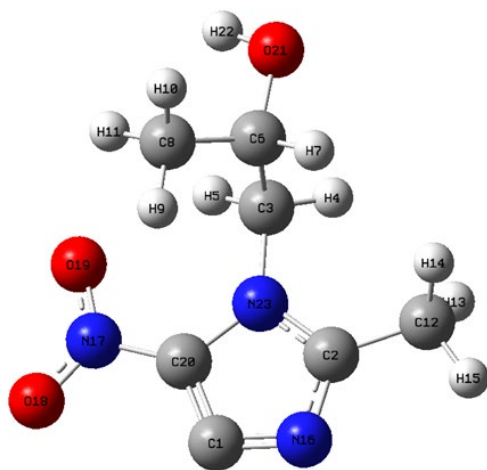


Figure 1: Secnidazole structure (up) the planar structure, (down) the 3D structure.

2. Material and Methods

2.1. Computational Method

For all kinds of calculations, the Gaussian 09 software package [19] with a personal computer was used by applying the Becke, 3-parameter, Lee-Yang-Parr (B3LYP) correlational functional with the cc-pVDZ basis and DFT method for the secnidazole molecule. In the first place, the geometries of the SNZ were optimized with the aforementioned level theory and basis sets. Negative frequency absence confirms that the optimized geometry is in the molecular state of the lowest energy. Then frontier orbitals (FMOs), FT-IR spectrum, ¹H NMR and ¹³C NMR spectra, UV-vis spectra in the gas phase and several solvents, and MPE of the titled compound were determined by the aforementioned model method. In addition, the dipole moment, solvation energies, and molecular properties were computed by implementing the Solvation Model on Density (SMD) [17, 20] in several solvents such as water, DMSO, nitromethane, acetone, and THF. All solvation calculations were done with optimized structures in the solution phase.

The molecular electrostatic potential has been calculated by the B3LYP/cc-pVDZ G model method in order to analyze

the reactive sites of the secnidazole molecule. At such a given point $r(x, y, z)$ in a molecule's vicinity, the $V(r)$ (MEP) is expressed in terms of the interaction energy between both the electric charge produced from electrons and nuclei of the molecule and a proton (positive test charge) located at r . The $V(r)$ values for the system studied were determined using the equation 1 as stated earlier [21], in which the charge of nucleus A is denoted by Z_A and its position is R_A , the molecular electron density function and the dummy integration variable are represented by $q(r)$ and r , respectively.

$$V(r) = \sum_A \frac{Z_A}{|R_A - r|} - \int \frac{\rho(r')}{|r' - r|} dr' \quad (1)$$

3. Results and Discussion

3.1 Molecular Geometry

The optimized molecular parameters such as the bond lengths and the bond angles of the secnidazole molecule were computed using the B3LYP/cc-pVDZ method, which are listed in Table 1. The molecular structure of the titled compound is presented in Fig. 1. The bond length of C1-C20 in the aromatic ring is calculated to be 1.3801 \AA which is the smallest bond length of a C-C bond in the titled molecule. While the C3-C6 bond length is found to be maximum (1.546 \AA) by comparing it to other C-C bond lengths in the secnidazole molecule, this may be due to the presence of oxygen and nitrogen atoms in the adjacent position. The C-N bond length is calculated between $1.315 - 1.4686 \text{ \AA}$ in which C3-N23 is found to be maximum by comparison to others C-N bond lengths. The bond length of O21-H22 is measured to be the smallest bond length in the titled compound which is equal to 0.9702 \AA . The bond length of N-O is computed between $1.225 - 1.4233 \text{ \AA}$. The C-H bond length is calculated between $1.0953 - 1.1029 \text{ \AA}$. The variation of bond angles is shown in table 1. The C1-C20-N17 bond angle is calculated to be the maximum value, which is found to be 128.029° while the minimum bond angle is calculated for C7-C6-O21 to be 104.458° . The bond angle of H-C-H is computed between $107.516^\circ - 109.081^\circ$.

Table 1 Calculated bond length and bond angle of secnidazole molecule with B3LYP/ cc-pVDZ model method.

| SI. No | Bond | Bond length (Å) | SI. No | Bond | Bond Angle (°) | SI. No | Bond | Bond Angle (°) |
|--------|---------|-----------------|--------|-------------|----------------|--------|-------------|----------------|
| 1 | C1-N16 | 1.315 | 1 | N16-C1-C20 | 112.104 | 24 | C2-C12-H14 | 112.300 |
| 2 | C1-C20 | 1.380 | 2 | C12-C2-N16 | 123.964 | 25 | C2-C12-H15 | 108.064 |
| 3 | C2-C12 | 1.492 | 3 | C12-C2-N23 | 124.479 | 26 | H13-C12-H14 | 107.605 |
| 4 | C2-N16 | 1.346 | 4 | N16-C2-N23 | 111.540 | 27 | C13-C12-H15 | 108.538 |
| 5 | C2-N23 | 1.367 | 5 | H4-C3-H5 | 108.815 | 28 | H14-C12-H15 | 108.645 |
| 6 | C3-H4 | 1.099 | 6 | H4-C3-C6 | 108.185 | 29 | C1-N16-C2 | 105.976 |
| 7 | C3-H5 | 1.095 | 7 | H4-C3-N23 | 107.780 | 30 | O18-N17-O19 | 124.769 |
| 8 | C3-C6 | 1.546 | 8 | H5-C3-C6 | 109.923 | 31 | O18-N17-C20 | 116.571 |
| 9 | C3-N23 | 1.469 | 9 | H5-C3-N23 | 107.464 | 32 | O19-N17-C20 | 118.659 |
| 10 | C6-C7 | 1.104 | 10 | C6-C3-N23 | 114.538 | 33 | C1-C20-N17 | 128.029 |
| 11 | C6-C8 | 1.525 | 11 | C3-C6-C7 | 108.496 | 34 | C1-C20-N23 | 104.988 |
| 12 | C6-O21 | 1.423 | 12 | C3-C6-C8 | 114.534 | 35 | N17-C20-N23 | 126.933 |
| 13 | C8-H9 | 1.102 | 13 | C3-C6-O21 | 107.470 | 36 | C6-O21-H22 | 107.495 |
| 14 | C8-H10 | 1.101 | 14 | C7-C6-C8 | 109.065 | 37 | C2-N23-C3 | 125.135 |
| 15 | C8-H11 | 1.102 | 15 | C7-C6-O21 | 104.458 | | | |
| 16 | C12-H13 | 1.103 | 16 | C8-C6-O21 | 112.283 | | | |
| 17 | C12-H14 | 1.102 | 17 | C6-C8-H9 | 111.603 | | | |
| 18 | C12-H15 | 1.097 | 18 | C6-C8-H10 | 109.358 | | | |
| 19 | N17-O18 | 1.225 | 19 | C6-C8-H11 | 111.092 | | | |
| 20 | N17-O19 | 1.239 | 20 | H9-C8-H10 | 108.105 | | | |
| 21 | N17-C20 | 1.423 | 21 | H9-C8-H11 | 107.516 | | | |
| 22 | C20-N23 | 1.405 | 22 | H10-C8-H11 | 109.081 | | | |
| 23 | O21-H22 | 0.970 | 23 | C2-C12-OH13 | 111.594 | | | |

3.2 Frontier Molecular Orbital (FMO) and UV-Vis Analysis

In chemistry, the concept of the highest occupied molecular orbital (HOMO) and the lowest unoccupied molecular orbital (LUMO) is crucial. Frontier orbitals are named for the fact that they are located at the outermost boundaries of the electrons in molecules. The theory of molecular orbitals is widely used to describe chemical behavior and molecular stability [22]. The HOMO-LUMO gap, also known as the band gap, can reveal a molecule's reactivity, structural, and physical properties [23]. Because the HOMO-LUMO orbital pair has the lowest energy of any pair of orbitals in the

molecule, they can interact more strongly than other pairs. As a result, molecules with large HOMO-LUMO gaps tend to be unreactive and stable, whereas those with small gaps tend to be reactive. The secnidazole molecule's molecular orbitals with the gap are shown in Figure 2. The HOMO energy is found to be -7.180eV, while the LUMO value is found to be -2.450eV for the gas phase. The band gap is found to be 4.730eV for the gas phase. Secnidazole is reactive in nature, as evidenced by the energy gap values. The HOMO-LUMO energy gap has been proven to show bioactivity from intramolecular charge transfer [24].

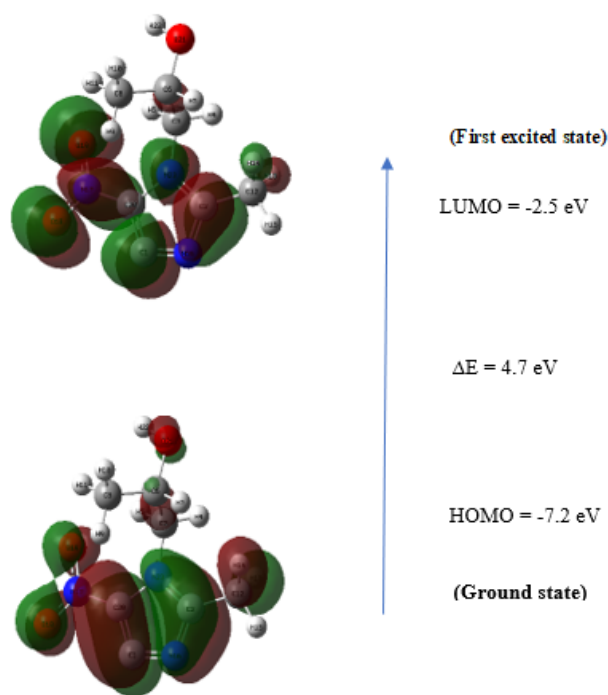


Figure 2 Contour diagram of frontier orbitals which is computed in the gas phase at B3LYP/cc-pVDZ level theory of the secnidazole molecule.

3.3 Molecular Electrostatic Potential (MEP) Surface Analysis

MEP enables the visualization of various molecularly charged regions. Information about the distribution of charges is used to evaluate how molecules interact with each other, and it can be used for predicting the reactivity and behavior of molecules [25]. The electrophilic attack in the MEP indicates the red and the nucleophilic attack is blue. The electrical potential decreases from the blue color to the red one (blue > green > red) [22]. In addition, the red color represents an area rich in electrons, while a neutral place is a green color, and the region of the electron deficient is represented by the blue color.

The MEP surface of the secnidazole molecule is shown in Figure 3. As per the different colors of the MEP region, the region of negative potential is observed near oxygen and nitrogen atoms; on the other hand, the region of positive potential is distributed over hydrogen atoms and ring systems as expected. The other parts seemed to be neutral. The region of positive potential near the hydrogen atoms and ring system shows the acceptor nature, while the region of negative potential near the oxygen atom and the nitrogen atom of the amino group shows the donor nature. The region of the negative potential is favorable

for lone pair interactions and hydrogen bonding interactions.

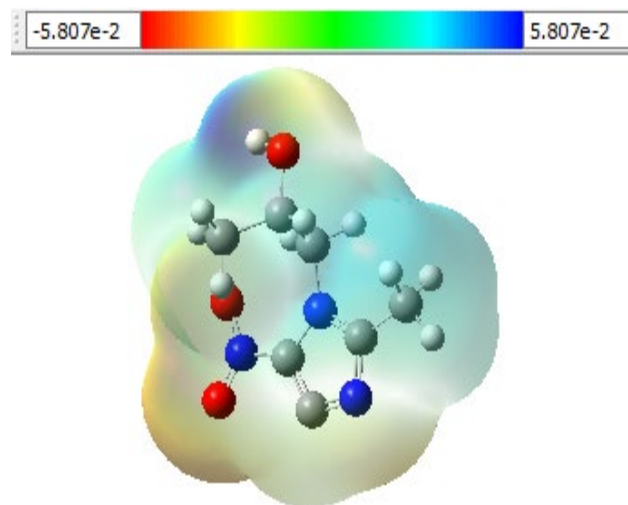


Figure 3 Electrostatic Potential Surface (ESP) and total electron density of secnidazole compound are mapped which is computed at B3LYP/cc-pVDZ level theory in the gas phase.

3.4. Mulliken Atomic Charge Distribution

In the use of calculations of quantum mechanics in molecular systems, the computation of Mulliken atomic charges plays a key role [22]. The Mulliken atomic charge uses to describe the processes of equalization of electronegativity and the mechanism of charge transfer in chemical reactions [26]. It influences lots of the properties, like electronic structure, dipole moment, and polarizability, of a molecule [22]. So, the charge distribution of the secnidazole compound was calculated by using Mulliken's analysis with the DFT method at the B3LYP/cc-pVDZ level of theory and is shown in Table 2. The molecule's overall charge is zero, according to the calculations, nitrogen and oxygen atoms have a delocalized negative charge. In SZN molecule, the atoms (N16 and N23) located in the ring system are the ones possess the smallest negative charges. Although the molecule's hydrogen atoms all have positive charges, oxygen atoms O8 and O9 have very similar negative charges. The nitrogen atoms N17 and N23 connected to carbon atoms C3 and C20 have more positive charges because of their electronegative nature [27]. Hydrogen atoms linked to carbon atoms on the outside of the ring have similar positive charge values. Hydrogen bonding may be the cause of the highest charge values seen for H22, as should be noted.

Table 2 Mulliken atomic charge distribution of secnidazole molecule which calculated at B3LYP/cc-pVDZ level of theory.

| Atom | Charge (C) |
|------|------------|
| C1 | -0.019 |
| C2 | 0.079 |
| C3 | 0.118 |
| H4 | 0.030 |
| H5 | 0.042 |
| C6 | 0.041 |
| H7 | 0.011 |
| C8 | 0.001 |
| H9 | 0.031 |
| H10 | 0.031 |
| H11 | 0.032 |
| C12 | 0.035 |
| H13 | 0.060 |
| H14 | 0.056 |
| H15 | 0.057 |
| N16 | -0.169 |
| N17 | 0.179 |
| O18 | -0.239 |
| O19 | -0.281 |
| C20 | 0.215 |
| O21 | -0.256 |
| H22 | 0.143 |
| N23 | -0.196 |

3.5. Vibrational Assignments

Vibrational measurements are important in organic samples for analysing structural changes in the material of interest. The vibrational spectrum analysis can also be performed to see if the solvents are still present or have evaporated completely during the drying process [28, 29]. However, in this study, the vibrational spectra of the secnidazole molecule in the gas phase are analysed using DFT/B3LYP methods and the cc-pVDZ basis set. Infrared absorption was used to investigate the structural conformation of secnidazole.

The computed IR spectra of the title compound are shown in Figure 4. In the secnidazole spectra, the absorption peaks are distinct. In compounds with an aromatic ring, the C-H stretching vibrations have a frequency range of 3000–3100 cm^{-1} [30–32]. The C-H stretching modes in the aromatic

rings of the named molecule are responsible for the absorption band seen at 3088 cm^{-1} in the IR spectrum. Similarly, in the vibrational assignments given in Figure 4, the calculated bands above 3000 cm^{-1} are bands that belong to the C-H stretching modes of aromatic rings (3744 cm^{-1}). In the area of 1000–1600 cm^{-1} , the C-H in-plane bending modes also appear combined with other bands, while the C-H out-of-plane bending ones are observed in a range of 650–1000 cm^{-1} . The observed bands at 1104 and 1376 cm^{-1} can be attributed to the C-H in-plane bending vibrations, while at 808 cm^{-1} the C-H out-of-plane bending bands may be seen. One of the most characterized bands of Schiff bases is N=C stretching mode for the phenol-imine form, which appears near 1620 cm^{-1} [33, 34]. The absorption band as the medium peak at 1616 cm^{-1} of the titled compound is corresponded to N=C stretching mode [33, 34].

Absorption bands in the range of 1400–1650 cm^{-1} are frequently produced by ring C-C stretching vibration. The ring C-C stretching vibration can be correlated to the observed band at 1464 cm^{-1} [35-37].

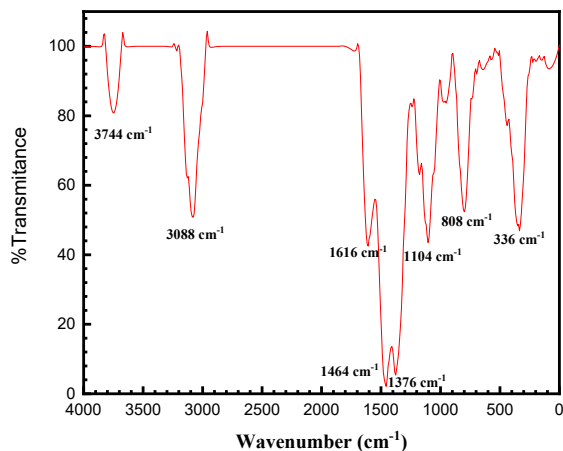


Figure 4 FTIR spectrum of secnidazole compound in the range (3500-0 cm^{-1}).

3.6. Analysis of NMR Chemical Shift

Nuclear magnetic resonance (NMR) spectroscopy helps us to analyze isotopic chemical changes, to describe relative ionic compounds, to measure precise magnetic properties, and to identify accurate molecular structural estimates. [37]. So that, the values of the chemical shift of the H^1 and C^{13} NMR of the secnidazole molecule were computed by the DFT/B3LYP methods at the cc-pVDZ basis set. The calculated H^1 and C^{13} NMR isotropic chemical shift values of the titled molecule are given in Table 3.

In the spectrum of C^{13} NMR chemical shift, resonance signals at 150–200 ppm and 100–150 ppm will provide aromatic carbons and carbons, carbons and alkene with a sp^2 hybridization, respectively. Nevertheless, the C^{13} NMR signals of methylene carbons and methyl arise in 10-60 ppm region in general [37]. The chemical shift values of carbon-13 for C1, C2 and C20 atoms which are bonded to the electronegative nitrogen atom are calculated to be in the range of 205.84 – 111.63 ppm. While the values of the carbon-13 NMR shift of C6, C3, C8 and C12 are calculated in 59.23 - 4.77 ppm regions. The H^1 NMR chemical shift for hydrogen (H) atoms of the titled molecule was given a resonance signal at the interval of 0.11 – 5.38 ppm. The calculated H-1 and C-13 NMR chemical shifts are shown in Figure 5.

Table 3 The computed chemical shifts of H^1 and C^{13} NMR of the secnidazole molecule at B3LYP/ cc-pVDZ level theory.

| Atoms | $\delta_{calc.}$ Ppm | Atoms | $\delta_{calc.}$ Ppm |
|-------|-------------------------|-------|-------------------------|
| C1 | 205.84 | H5 | 5.38 |
| C2 | 124.71 | H7 | 4.19 |
| C20 | 111.63 | H4 | 4.06 |
| C6 | 59.23 | H15 | 2.80 |
| C3 | 43.11 | H13 | 2.71 |
| C8 | 10.96 | H14 | 2.62 |
| C12 | 4.77 | H10 | 1.72 |
| | | H11 | 1.65 |
| | | H9 | 1.45 |
| | | H22 | 0.11 |

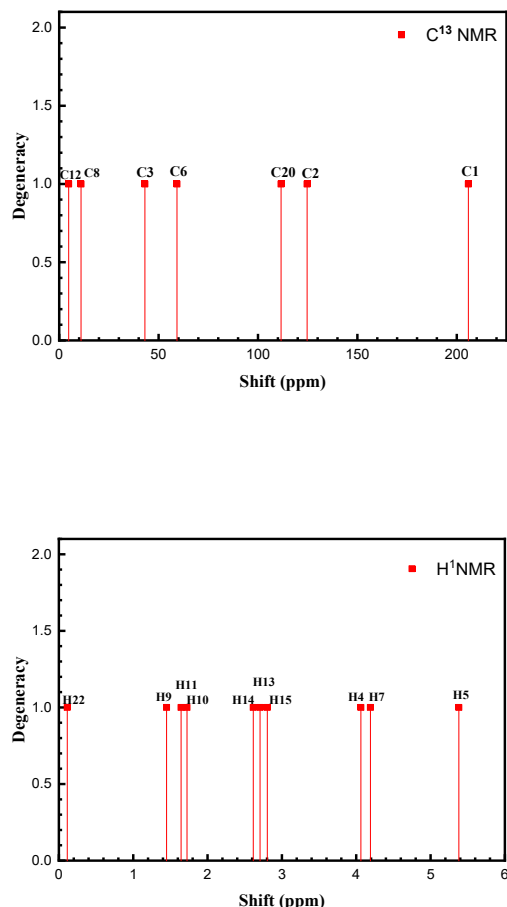


Figure 5 The calculated C^{13} and H^1 NMR chemical shifts (TMS B3LYP/6-311+G (2d, p) GIAO) of secnidazole compound with DFT/B3LYP methods at cc-pVDZ.

3.7. UV- Vis Spectroscopy

UV- visible spectroscopy can be considered as one of the basic and most effective optical techniques for studying the electronic and optical properties of nanomaterials like polymers, semiconductors, organic light-emitting, and organic materials [38]. The spectrum represents the sample's basic electronic properties. The calculated UV-visible spectra of secnidazole with DFT/B3LYP methods at cc-pVDZ for five different solvents such as water, DMSO, nitromethane, acetone, and THF are shown in Figure 6. According to Figure 6, three peaks are located almost in the region of near-ultraviolet (200-400 nm). As seen in the figure the values of maximum absorption wavelengths (λ_{max}) for the solutions of secnidazole were found at 296 nm (water), 267 nm (DMSO), 247 nm (nitromethane, acetone, and THF), respectively, which reveals that the λ_{max} is become smaller with decreasing the dielectric constants of the solvents. The values of the molar extinction coefficient (ϵ) of solutions of secnidazole are found to be unstable for

the aforementioned solvents. The values of maximum molar extension coefficient (ϵ_{max}) at λ_{max} (296 nm, 267nm, 247nm) of secnidazole compound for aforementioned solvents were found to be 10650 $Lmol^{-1} cm^{-1}$, 10761 $Lmol^{-1} cm^{-1}$ and 10975 $Lmol^{-1} cm^{-1}$, respectively. So, the highest value of ϵ_{max} was found for nitromethane, acetone, and THF while the lowest one was for water. The theoretical UV-Vis spectra of secnidazole are shown in Figure 6. We have calculated the absorption peak (λ_{max}) and oscillator strength (f) in order to understand the nature of the electronic transition.

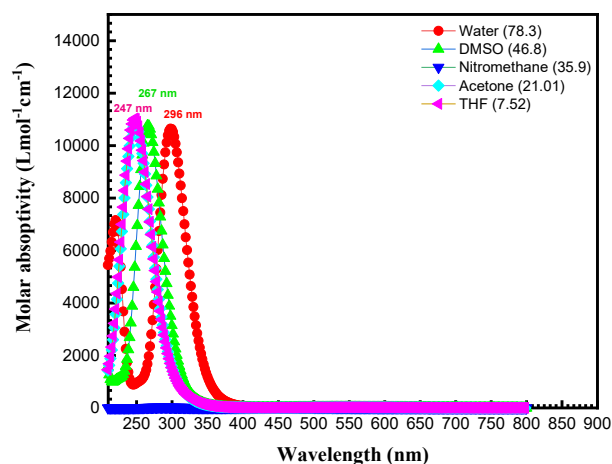


Figure 6 The plots of molar absorptivity coefficient (ϵ) versus of wavelength (λ) of secnidazole molecule for several solvents.

3.8. Solvation Free Energy

In five different solvent systems, namely water, DMSO, nitromethane, acetone, and THF, the proposed SMD model was performed for calculating the solvent-free energy. The calculations of solvation free energy (ΔG) are performed based on the following equation:

$$\Delta G = G(Sol) - G(gas)$$

In which

$G(gas)$ = (electronic energy + thermal free energy) in the gas phase

$G(sol)$ = (electronic energy + thermal free energy) insolvent
From a higher value to a lower value of the dielectric constant, the free energy continuously increased, i.e. with the declining solvent polarity, the solvation energy rises, which is shown in Table 4 and Figure 7.

This results in the varying interaction degrees and thus, HOMO-LUMO orbital stabilization by the various solvents.

It is obvious from Table 6 and Figure 11 that the HOMO-LUMO band gap energy increases as the solvent's polarity

decreases, interactions to a higher degree are suggested for secnidazole with declining medium polarity.

Table 4 Secnidazole solvation free energy (kJ/mol) and dipole moment (D) in five different solvents using the DFT method and B3LYP with the cc-pVDZ basis set and SMD model.

| Medium (dielectric constant) | Solvation free energy (kJ/mol) | Dipole moment (D) |
|------------------------------|--------------------------------|-------------------|
| Gas Phase | - | 4.41 |
| Water (78.3) | -33.8 | 6.29 |
| DMSO (46.8) | -44.83 | 6.01 |
| Nitromethane (35.9) | -47.72 | 6.00 |
| Acetone (21.01) | -52.65 | 5.71 |
| THF (7.52) | -52.61 | 5.70 |

3.9. Dipole Moment

It is expected that the dipole moment is greater in solution than the related dipole moment in the gas phase. The dipole moments were calculated in both the gas phase and various solvents (water, DMSO, nitromethane, acetone and THF) at the B3LYP level of theory with the cc-pVDZ basis set applying the SMD solvation model (Table 4). From a lower value to a higher value of the dielectric constant, the dipole moment was continuously raised i.e. by the increase of solvent polarity the dipole moment increased as shown in Figure 8.

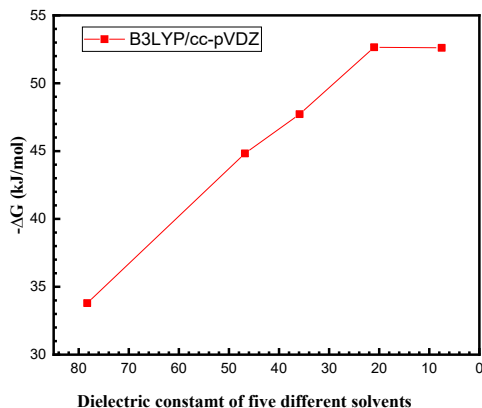


Figure 7 Solvent polarity effect on solvation free energy (kJ/mol) of secnidazole.

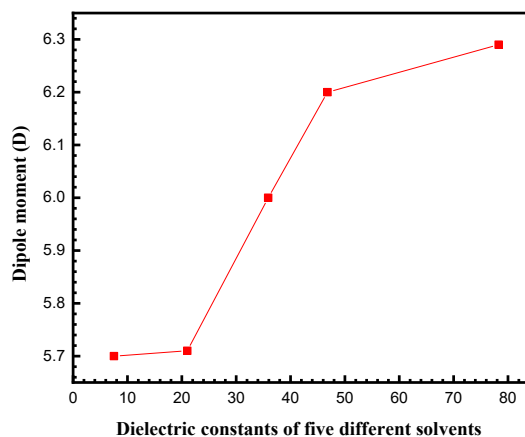


Figure 8 Solvent polarity effect on dipole moment (D) of secnidazole.

3.10. Polarizability and First-Order Hyperpolarizability

A molecule's distortion in an electric field can be measured by polarizability. By implementing the following equation, the polarizability (α) has been calculated.

$$\alpha = \frac{1}{3}(\alpha_{xx} + \alpha_{yy} + \alpha_{zz})$$

Molecular interaction strength and a system's optical properties can be determined by polarizability [12]. A molecule that has a small gap between HOMO and LUMO, is highly polarizable and has a high level of chemical reactivity, a low level of kinetic stability, as well as a high level of electro-optic, reflect is called a soft molecule [39]. Table 5 and Figure 9 present the calculated polarizability of the title molecule, which shows that polarizability continuously increases from a lower value to a higher value of the dielectric constant. This is due to a varying degree of solvent interactions with the HOMO -LUMO orbitals of secnidazole. Table 6 and Figure 11 demonstrate that the energy gap of HOMO-LUMO decreases as the solvent dielectric constant increases, Thus, the molecule becomes more reactive to increase solvent polarity. However, Secnidazole's polarizability ranged from 80.41 to 81.06 a.u.in various solvents.

The nonlinear optical activity can be measured by the first-order hyperpolarizability like β_{vec} (β vector), β_{II} (β parallel), β_{tot} (β total) which is a tensor of the third rank and can be represented ed by a $(3 \times 3 \times 3)$ matrix. The Kleinman symmetry scales down the (27) components of the (three-dimensional) 3D matrix to become 10 components [40]. The

GAUSSIAN program gives the 10 components of this three-dimensional matrix like $\beta_{yyz}, \beta_{xxx}, \beta_{xzz}, \beta_{xyy}, \beta_{zzz}, \beta_{xyz}, \beta_{yyy}, \beta_{xxz}, \beta_{yxx}, \beta_{yzz}$, sequentially. One can use these for calculating all x, y, and z components of β .

In this study, the β_{tot} for five different solvents is reported and listed in Table 5. The β_{tot} components can be calculated with the following equation.

$$\beta_{tot} = (\beta_x^2 + \beta_y^2 + \beta_z^2)^{1/2}$$

Where,

$$\beta_x = \beta_{xxx} + \beta_{xyy} + \beta_{xzz}$$

$$\beta_y = \beta_{yyy} + \beta_{xxy} + \beta_{yzz}$$

$$\beta_z = \beta_{zzz} + \beta_{xxz} + \beta_{yyz}$$

From a lower value to a higher value of solvent dielectric constant, the first-order hyperpolarizability has risen, i. e, as shown in Figure 10, the first-order hyperpolarizability increased as the solvent polarity increased. The hyperpolarizability difference was between 65.91 and 70.65 a.u. in the various solvents.

Table 5 The effect of Medium on polarizability and first-order hyperpolarizability both with (a. u.).

| Medium (dielectric constant) | α_{xx} | α_{yy} | α_{zz} | α_{tot} | β_x | β_y | β_z | β_{tot} |
|------------------------------|---------------|---------------|---------------|----------------|-----------|-----------|-----------|---------------|
| Gas Phase | 88.98 | 76.74 | 73.53 | 79.75 | -47.24 | -17.19 | -18.88 | 53.69 |
| Water (78.3) | 93.19 | 76.94 | 73.04 | 81.06 | -66.19 | -5.820 | -24.01 | 70.65 |
| DMSO (46.8) | 91.70 | 77.02 | 73.25 | 80.69 | -63.95 | -10.80 | -23.90 | 69.5 |
| Nitromethane (35.9) | 91.81 | 77.00 | 73.21 | 80.67 | -64.13 | -10.39 | -23.85 | 69.21 |
| Acetone (21.01) | 91.64 | 76.95 | 73.22 | 80.61 | -63.40 | -10.61 | -23.54 | 68.45 |
| THF (7.52) | 91.15 | 76.84 | 73.24 | 80.41 | -60.89 | 11.33 | -22.55 | 65.91 |

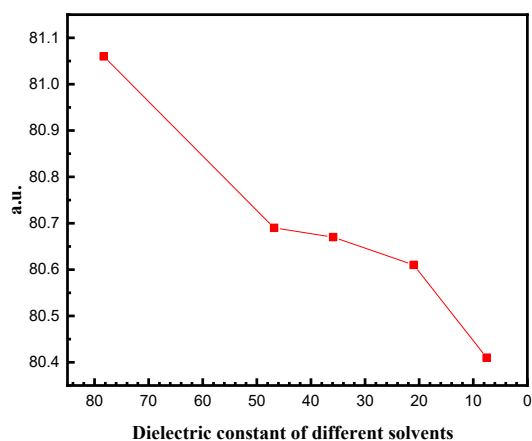


Figure 9 Solvent polarity effect on polarizability.

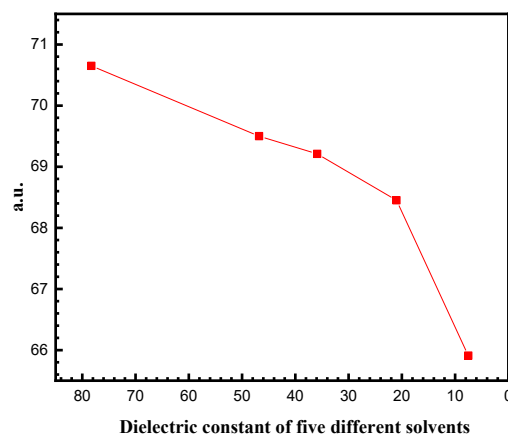


Figure 10 Solvent polarity effect on the first-order hyperpolarizability.

3.11. Global Reactivity Descriptors

The HOMO-LUMO bandgap energy specifies the properties of the electrical transport of the molecule. The energy gap between HOMO and LUMO can be used for calculating the molecules' chemical reactivity descriptors such as chemical potential, hardness, electronegativity, softness, electronegativity, and electrophilicity index [41]. The HOMO- LUMO bandgap energy of secnidazole is shown in Table 6 and Figure 11.

For the molecules of the closed shell, the Koopman's theorem can be implemented for calculating the softness (S), chemical potential (μ), and electronegativity and hardness (η), using the following equations:

$$\eta = \frac{I - A}{2}$$

$$\mu = -\frac{I + A}{2}$$

$$\chi = \frac{I + A}{2}$$

$$S = \frac{1}{\eta}$$

In which A and I are electron affinity and the ionization potential of the compound, respectively and $A = -E_{LUMO}$, $I = -E_{HOMO}$.

Molecules with a large bandgap between HOMO and LUMO are referred to as hard molecules, while molecules with a small energy difference between HOMO and LUMO are known as soft molecules. Molecular stability is related to hardness and softness. A molecule with the smallest HOMO-LUMO band gap is highly reactive and vice versa. A molecule's electrophilic powers, such as electrophilicity index (ω) are defined by Parr et al. 1999 [42] which can be calculated by the following formula:

$$\omega = \frac{\mu^2}{2\eta}$$

The mentioned equation can be used for calculating hardness and chemical potential, as well as an electrophilicity index. This quantity of reactivity was used to consider the toxicity and site selectivity of different pollutants [43] Table 7 presents the molecular properties of secnidazole in both the gas phase and the various mediums. The electrophilicity index, electronegativity, and chemical potential of secnidazole were decreased, from polar to non-polar solvents (Figures 12 and 13).

In THF, there was a greater chemical potential, electrophilicity index, and electron negativity than in acetone. While chemical hardness has been increased by decreasing solvent polarity, the opposite relationship has been found for chemical softness.

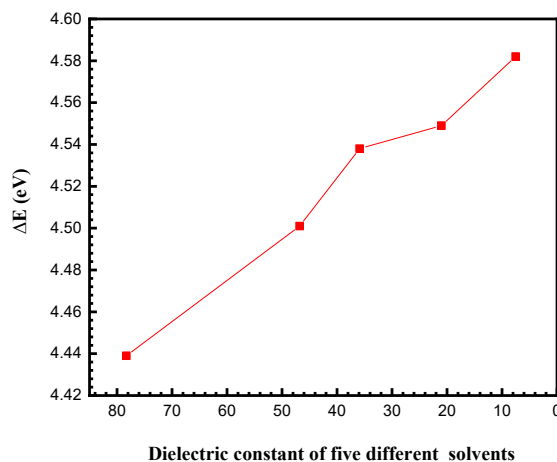


Figure 11 Solvent polarity effect on HOMO-LUMO bandgap energy of secnidazole.

Table 6 The (HOMO and LUMO) bandgap energy of secnidazole in five different solvents with SMD.

| Medium (Medium dielectric constant) | Molecular orbital energy (eV) | | |
|-------------------------------------|-------------------------------|--------|---------|
| | HOMO | LUMO | ΔE (eV) |
| Gas Phase | -7.180 | -2.450 | 4.730 |
| Water (78.3) | -6.974 | -2.535 | 4.439 |
| DMSO (46.8) | -6.888 | -2.341 | 4.501 |
| Nitromethane (35.9) | -6.894 | -2.356 | 4.538 |
| Acetone (21.01) | -6.903 | -2.354 | 4.549 |
| THF (7.52) | -6.938 | -2.357 | 4.582 |

Table 7 The effect of medium on molecular properties of secnidazole, in which the Chemical hardness, Softness, Chemical potential, Electronegativity, Electrophilicity index are represented by η , S , μ , χ and ω , respectively.

| Medium (dielectric constant) | η (eV) | S (eV) | μ (eV) | χ (eV) | ω (eV) |
|------------------------------|-------------|----------|------------|-------------|---------------|
| Gas Phase | 2.365 | 0.4228 | -4.82 | 4.82 | 4.91 |
| Water (78.3) | 2.220 | 0.4505 | -4.76 | 4.76 | 5.10 |
| DMSO (46.8) | 2.250 | 0.4443 | -4.67 | 4.67 | 5.09 |
| Nitromethane (35.9) | 2.269 | 0.4407 | -4.66 | 4.66 | 5.07 |
| Acetone (21.01) | 2.275 | 0.4396 | -4.63 | 4.63 | 4.71 |
| THF (7.52) | 2.291 | 0.4365 | -4.65 | 4.65 | 4.72 |

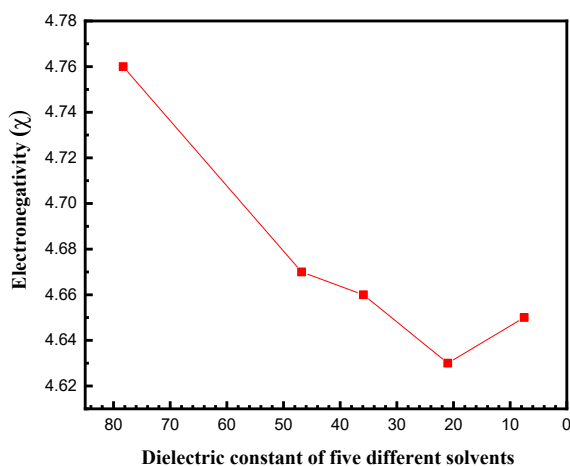


Figure 12 Solvent polarity effect on the electronegativity of secnidazole.

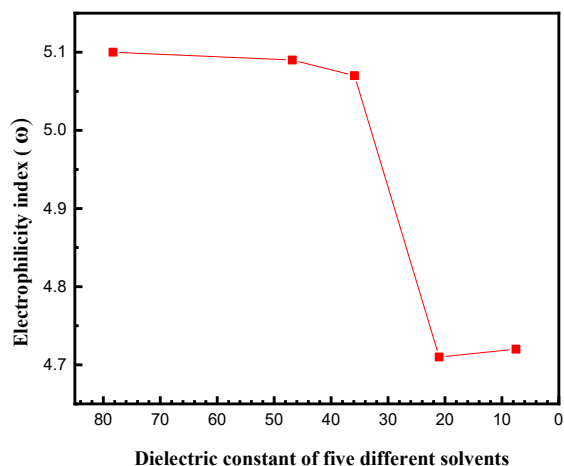


Figure 13 Solvent polarity effect on electrophilicity index of secnidazole.

4. Conclusion

In this study, the structural and spectroscopic properties of secnidazole compound in various solvents were studied theoretically using DFT/B3LYP methods at cc-pVDZ level theory. The molecular geometry parameters, frontier molecular orbitals, molecular electrostatic potential, and Mulliken atomic charge distribution of the titled compound have been reported and discussed. In addition, the spectroscopic properties of the compound were investigated by implementing spectroscopic techniques such as H^1 NMR

and C^{13} , UV-Vis and FTIR with the aforementioned level of theory. The technique of solution was used to study the optical properties of the titled molecule. In addition, the effect of medium on dipole moment, free energies, and properties of the molecule were computed by applying the aforementioned method. The free energy was gradually increased by decreasing the solvent dielectric constant. With the increase of solvent polarity, the polarizability, dipole moment, and hyperpolarizability of secnidazole have steadily increased. With going from polar to non-polar solvent, the electrophilicity index, electronegativity, and chemical potential all decreased. In the THF solvent, secnidazole had a greater electronegativity, chemical potential, and electrophilicity index than acetone. However, chemical hardness has been increased with lower solvent polarity, and an inverse relation has been found for chemical softness. Consequently, secnidazole can be considered more reactive and not stable in a polar solvent, and the polarizability and chemical softness in five different solvents make it clear. The results of this study can be helpful in finding theoretical evidence for secnidazole in intermediate reactions and pharmaceuticals.

References

- [1] X.-S. Huang, L.-S. Wang, Y. Yin, W.-M. Li, M. Duan, W. Ran, *et al.*, "Synthesis, Characterization and Bioactivity Research of a Derivative of Secnidazole: 1-(2-Chloropropyl)-2-methyl-5-nitro-1 H-imidazole," *Journal of Chemical Crystallography*, vol. 41, pp. 1360-1364, 2011.
- [2] S. Khan, M. Haseeb, M. H. Baig, P. S. Bagga, H. Siddiqui, M. Kamal, *et al.*, "Improved efficiency and stability of secnidazole—An ideal delivery system," *Saudi journal of biological sciences*, vol. 22, pp. 42-49, 2015.
- [3] A. B. Rivera, R. G. Hernández, H. N. de Armas, D. M. C. Elizástegi, and M. V. Losada, "Physico-chemical and solid-state characterization of secnidazole," *Il Farmaco*, vol. 55, pp. 700-707, 2000.
- [4] M. Bakshi and S. Singh, "Establishment of inherent stability of secnidazole and development of a validated stability-indicating HPLC assay method," *JOURNAL OF PHARMACY AND PHARMACOLOGY*, vol. 55, pp. 16-16, 2003.
- [5] T. Saffaj, M. Charrouf, A. Abourriche, Y. Aboud, A. Bennamara, and M. Berrada, "Spectrophotometric determination of metronidazole and secnidazole in pharmaceutical preparations based on the formation of dyes," *Dyes and pigments*, vol. 70, pp. 259-262, 2006.
- [6] H. Novoa, R. González, A. Dago, R. Pomés, and N. Li, "Estructura cristalina del (hidroxi-2-propil)-1-metil-2-nitro-5-imidazol hemihidratado," *ReV. CENIC Ciencias Quim*, vol. 28, p. 89, 1997.
- [7] E. Li-Chan, J. M. Chalmers, and P. R. Griffiths, *Applications of vibrational spectroscopy in food science*: John Wiley & Sons, 2010.
- [8] S. Mishra, D. Chaturvedi, P. Tandon, V. Gupta, A. Ayala, S. Honorato, *et al.*, "Molecular structure and vibrational spectroscopic investigation of secnidazole using density functional theory," *The Journal of Physical Chemistry A*, vol. 113, pp. 273-281, 2009.
- [9] B. P. Bezerra, J. C. Fonseca, Y. S. de Oliveira, M. S. A. de Santana, K. F. Silva, B. S. Araújo, *et al.*, "Phase transitions in secnidazole: Thermal stability and polymorphism studied by X-ray powder diffraction, thermal analysis and vibrational spectroscopy," *Vibrational Spectroscopy*, vol. 86, pp. 90-96, 2016.
- [10] P. Lakshmi Praveen and D. Ojha, "Substituent and solvent effects on UV-visible absorption spectra of liquid crystalline disubstituted biphenylcyclohexane derivatives—a computational approach," *Crystal Research and Technology*, vol. 47, pp. 91-100, 2012.
- [11] M. F. Khan, R. B. Rashid, M. A. Hossain, and M. A. Rashid, "Computational study of solvation free energy, dipole moment, polarizability, hyperpolarizability and molecular properties of Betulin, a constituent of *Corypha taliera* (Roxb.)," *Dhaka University Journal of Pharmaceutical Sciences*, vol. 16, pp. 1-9, 2017.
- [12] M. Targema, N. O. Obi-Egbedi, and M. D. Adeoye, "Molecular structure and solvent effects on the dipole moments and polarizabilities of some aniline derivatives," *Computational and Theoretical Chemistry*, vol. 1012, pp. 47-53, 2013.
- [13] A. HSSAIN, "Serotonin: Structural Characterization and Determination of The Band Gap Energy," *Journal of Physical Chemistry and Functional Materials*, vol. 2, pp. 54-58.
- [14] A. Jayaprakash, V. Arjunan, S. P. Jose, and S. Mohan, "Vibrational and electronic investigations, thermodynamic parameters, HOMO and LUMO analysis on crotonaldehyde by ab initio and DFT methods," *Spectrochimica Acta Part A*:

- Molecular and Biomolecular Spectroscopy*, vol. 83, pp. 411-419, 2011.
- [15] L. A. OMER and R. O. ANWER, "Population Analysis and UV-Vis spectra of Dopamine Molecule Using Gaussian 09," *Journal of Physical Chemistry and Functional Materials*, vol. 3, pp. 48-58, 2020.
- [16] L. AHMED and O. Rebaz, "A theoretical study on Dopamine molecule," *Journal of Physical Chemistry and Functional Materials*, vol. 2, pp. 66-72, 2019.
- [17] A. V. Marenich, C. J. Cramer, and D. G. Truhlar, "Universal solvation model based on solute electron density and on a continuum model of the solvent defined by the bulk dielectric constant and atomic surface tensions," *The Journal of Physical Chemistry B*, vol. 113, pp. 6378-6396, 2009.
- [18] M. F. Khan, R. Rashid, M. M. Rahman, M. Al Faruk, M. M. RAHMAN, and M. A. RASHID, "Effects of solvent polarity on solvation free energy, dipole moment, polarizability, hyperpolarizability and molecular reactivity of aspirin," *Int. J. Pharm. Pharm. Sci*, vol. 9, pp. 217-221, 2017.
- [19] M. Frisch, G. Trucks, H. Schlegel, G. Scuseria, M. Robb, J. Cheeseman, *et al.*, "Gaussian 09, Revision D. 01, 2009, Gaussian," *Inc., Wallingford CT*, 2009.
- [20] M. F. Khan, R. B. Rashid, M. Y. Mian, M. S. Rahman, and M. A. Rashid, "Effects of Solvent Polarity on Solvation Free Energy, Dipole Moment, Polarizability, Hyperpolarizability and Molecular Properties of Metronidazole," *Bangladesh Pharmaceutical Journal*, vol. 19, pp. 9-14, 2016.
- [21] P. Politzer and J. S. Murray, "The fundamental nature and role of the electrostatic potential in atoms and molecules," *Theoretical Chemistry Accounts*, vol. 108, pp. 134-142, 2002.
- [22] M. M. Borah and T. G. Devi, "Vibrational study and Natural Bond Orbital analysis of serotonin in monomer and dimer states by density functional theory," *Journal of Molecular Structure*, vol. 1161, pp. 464-476, 2018.
- [23] M. M. Borah and T. G. Devi, "The vibrational spectroscopic studies and molecular property analysis of l-Phenylalanine using quantum chemical method," *Journal of Molecular Structure*, vol. 1136, pp. 182-195, 2017.
- [24] K. Fukui, "The role of frontier orbitals in chemical reactions (Nobel Lecture)," *Angewandte Chemie International Edition in English*, vol. 21, pp. 801-809, 1982.
- [25] J. M. Seminario, *Recent developments and applications of modern density functional theory*: Elsevier, 1996.
- [26] A. D. Becke, "A new mixing of Hartree-Fock and local density-functional theories," *The Journal of chemical physics*, vol. 98, pp. 1372-1377, 1993.
- [27] R. G. Raman, "Spectroscopic and second harmonic generations studies of 5-Bromo-2-Methoxybenzonitrile by DFT," *Oriental Journal of Chemistry*, vol. 33, p. 3077, 2017.
- [28] N. Poad, S. Ngah Demon, M. Yahya, and N. Bidin, "Optical characteristics of ITO/NTCDA film for defence technology application," *Int. J. Curr. Res. Sci. Eng. Technol*, vol. 1, p. 262, 2018.
- [29] A. H. Hssain, B. Gündüz, A. Majid, and N. Bulut, "NTCDA Compounds of Optoelectronic Interest: Theoretical Insights and Experimental Investigation," *Chemical Physics Letters*, p. 138918, 2021.
- [30] N. Colthup, "Daly LH, and Wiberley, S," *E., Introduction to Infrared and Raman Spectroscopy*, Academic Press Inc., New York. N. Y, pp. 306-307, 1964.
- [31] L. Bellamy, "The infrared spectra of complex molecules 3 Wiley New York," *Search Google Scholar Export Citation*, 1975.
- [32] B. H. Stuart, *Infrared spectroscopy: fundamentals and applications*: John Wiley & Sons, 2004.
- [33] S. Miertuš, E. Scrocco, and J. Tomasi, "Electrostatic interaction of a solute with a continuum. A direct utilization of AB initio molecular potentials for the prevision of solvent effects," *Chemical Physics*, vol. 55, pp. 117-129, 1981.
- [34] M. Cossi, N. Rega, G. Scalmani, and V. Barone, "Energies, structures, and electronic properties of molecules in solution with the C-PCM solvation model," *Journal of computational chemistry*, vol. 24, pp. 669-681, 2003.
- [35] A. Abbas, S. Bahçeli, H. Gökçe, M. Bolte, S. Hussain, and M. K. Rauf, "Crystallographic structure and quantum chemical computations of 1-(3, 4-dimethylphenyl)-3-phenyl-5-(4-methoxyphenyl)-2-pyrazoline," *Spectrochimica Acta Part A: Molecular and Biomolecular Spectroscopy*, vol. 116, pp. 599-609, 2013.
- [36] H. Gökçe, O. Akyildirim, S. Bahçeli, H. Yükek, and Ö. G. Kol, "The 1-acetyl-3-

- methyl-4-[3-methoxy-4-(4-methylbenzoxo)benzylidenamino]-4, 5-dihydro-1H-1, 2, 4-triazol-5-one molecule investigated by a joint spectroscopic and quantum chemical calculations," *Journal of Molecular Structure*, vol. 1056, pp. 273-284, 2014.
- [37] T. Shimada, S. Hotta, and H. Yanagi, "Energy-transferred photoluminescence from thiophene/phenylene oligomer thin films," *Journal of luminescence*, vol. 128, pp. 457-461, 2008.
- [38] C. Orek, B. Gündüz, O. Kaygili, and N. Bulut, "Electronic, optical, and spectroscopic analysis of TBADN organic semiconductor: Experiment and theory," *Chemical Physics Letters*, vol. 678, pp. 130-138, 2017.
- [39] M. Targema, N. O. Obi-Egbedi, M. D. J. C. Adeoye, and t. Chemistry, "Molecular structure and solvent effects on the dipole moments and polarizabilities of some aniline derivatives," vol. 1012, pp. 47-53, 2013.
- [40] D. J. P. R. Kleinman, "Nonlinear dielectric polarization in optical media," vol. 126, p. 1977, 1962.
- [41] P. K. Chattaraj, B. Maiti, and U. Sarkar, "Philicity: a unified treatment of chemical reactivity and selectivity," *The Journal of Physical Chemistry A*, vol. 107, pp. 4973-4975, 2003.
- [42] R. G. Parr, L. v. Szentpaly, and S. J. J. o. t. A. C. S. Liu, "Electrophilicity index," vol. 121, pp. 1922-1924, 1999.
- [43] R. Parthasarathi, J. Padmanabhan, V. Subramanian, U. Sarkar, B. Maiti, and P. Chattaraj, "Toxicity analysis of benzidine through chemical reactivity and selectivity profiles: a DFT approach," *Internet Electronic Journal of Molecular Design*, vol. 2, pp. 798-813, 2003.